Conceptual design of a fixed wing hybrid UAV UUV platform

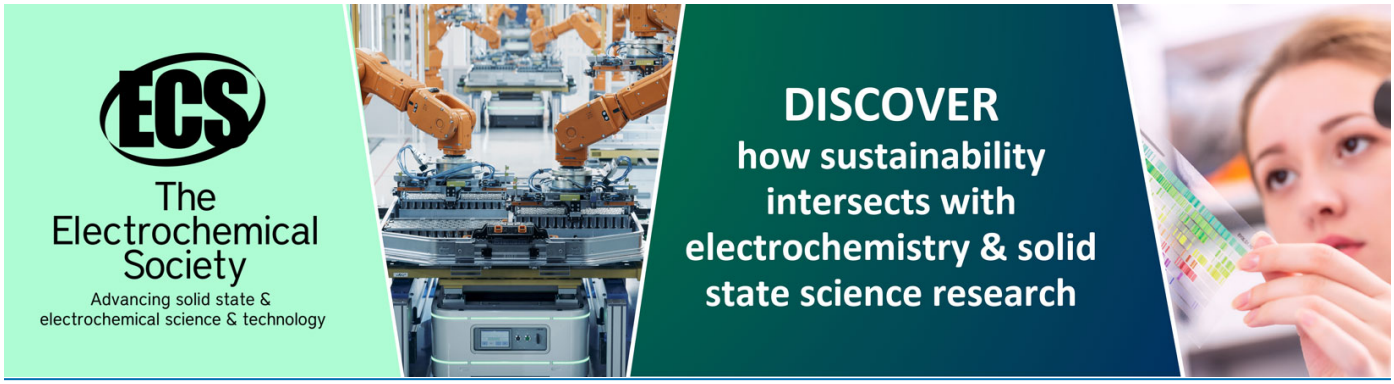

Conceptual design of a fixed wing hybrid UAV UUV platform

C Papadopoulos[1,2], S Vlachos[1,2] and K Yakinthos[1,2]

[1]Laboratory of Fluid Mechanics and Turbomachinery, Department of Mechanical Engineering, Aristotle University of Thessaloniki, Thessaloniki, 54124, Greece
[2]UAV integrated Research Center (UAV-iRC), Center for Interdisciplinary Research and Innovation (CIRI), Aristotle University of Thessaloniki, 57001, Thessaloniki, Greece
kyak@auth.gr

Abstract. In this work, the conceptual design methodology of a hybrid Unmanned Aerial Vehicle (UAV) – Unmanned Underwater Vehicle (UUV) platform is presented. As the mission complexity and the need for interoperability between different platforms grows more demanding by the day, hybrid platforms are becoming an essential solution. Hybrid UAV-UUVs can operate seamlessly and repeatedly in both the aerial and underwater environments, something that numerous animal species already execute in an optimized way. The design methodology starts with the review of the few available prototypes, creating initial design trends and continues with analytical calculations. These calculations are based on aircraft design textbooks and are modified to take into account the special characteristics of a hybrid platform, such as the means of transition between the water and the air. A Blended Wing Body (BWB) layout configuration is selected for the numerous aerodynamic advantages that it offers. The analytical calculations are then validated with the use of high fidelity CFD calculations. The results from the conceptual design phase indicate that the proposed methodology for hybrid UAV-UUV configurations provides a good design accuracy. Finally, the outcome of this methodology, which is a hybrid UAV-UUV platform is potentially the answer to the operational gap for missions that include both underwater and aerial environments.

Key words: UAV, UUV, Hybrid, BWB, Conceptual Design, Methodology, CFD

1. Introduction

The idea of Unmanned Vehicles (UVs) dates to the ancient times, with Archytas of Tarentum supposedly even creating the first known Unmanned Aerial Vehicle (UAV) around 350 BC. UVs and especially UAVs have seen a rapid development in the last decades, for both military and civil applications. Unmanned vehicles have many advantages, mainly arising from the lack of crew onboard. According to their operating environment, they are divided in aerial (UAV), underwater (UUV), surface (USV) and ground (UGV) vehicles. In nature, there are numerous animal species that execute multi-domain missions to hunt and survive, transitioning seamlessly between water and air. Bio-inspired designs and prototypes of manned multi-domain vehicles exist for over 100 years [1], but only the recent advancements of unmanned vehicles' technology made the concept feasible [2]. Potential applications of an Unmanned Aerial-Underwater Vehicle (UAUV) vary from search and rescue, intelligence-surveillance-reconnaissance (ISR) and border patrolling to ecosystem monitoring missions.

There are two categories of UAUVs, namely the ‘multi-rotor’ and the ‘fixed wing’ [1]. One of the first fixed wing UAUV design studies was conducted by a team of researchers in the Beihang University [3]. Their submersible UAV had coaxial counter rotating air propellers on the front and a single water propeller on the rear, retractable hollow wing and was designed to plunge-dive into the water and take-off vertically.

Air-to-water transition (ingress) may be performed either by water landing followed by a change in the buoyancy with a ballast system to reach the desirable mission depth or by plunge-diving. A series of partially featured UAUVs were developed in the Naval Research Laboratory of Washington, providing significant experimental results of the vehicle survivability during the plunge-diving ingress [4].On the other hand, water-to-air transition (egress), may be performed either with a fast, almost vertical, aquatic escape with the use of the propeller, or with an initial change of buoyancy to reach the water surface followed by a conventional hydroplane takeoff. An alternative egress procedure was demonstrated by Sidal et al. [5], who manufactured a prototype Aquatic Micro Aerial Vehicle (AquaMAV – figure 1a) that successfully achieved a fast egress using a water jet propulsion mechanism.

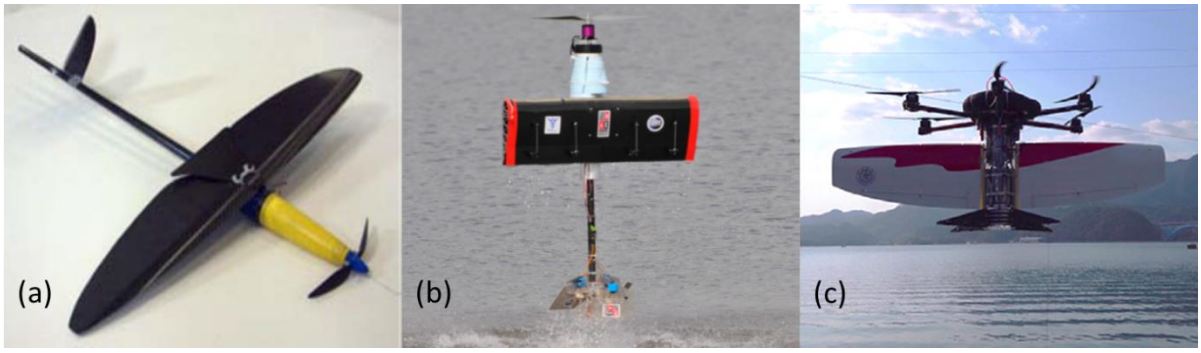

Figure. 1 Three examples of UAUVs: (a) AquaMAV [6] (b) EagleRay [7] (c) NEZHA III [8].

All the above-mentioned studies, verify the feasibility of various UAUV aspects. However, repeated bidirectional transitions through the two mediums is still a challenging task. Stewart et al. [7] demonstrated a hybrid UAUV (EagleRay – figure 1b) that can perform the complete operational cycle multiple times. A key component was the floodable wing, which enabled the rapid egress of the vehicle during a vertical takeoff maneuver. Lu et al. [8] designed and built a prototype UAUV which merges the design concepts of the fixed wing, the multirotor and the buoyancy system of underwater gliders, in order to provide a solution to the poor endurance capabilities of the existing UAUVs. Their second prototype (NEZHA III – figure 1c) demonstrated an outstanding capability of a 50-meter-depth dive.

The majority of the literature designs are conventional tube-and-wing configurations, mostly due to the simplicity for an initial proof-of-concept prototype. The novel but well-proven Blended Wing Body (BWB) layout though [9], could enhance the overall efficiency of the UAUV. Specifically, the BWB platform may offer up to 30% enhanced aerodynamic efficiency and a low wetted area to internal volume ratio, which may lead to a larger available volume used for additional payload or buoyancy tank.

Regarding the design procedure, Crouse et al. [10] presented many useful aspects of a multi-domain vehicle. While some steps of the design procedure are also addressed in the literature [11], there is yet to be specified a complete, step-by-step conceptual design methodology that also integrates aspects of the multi-domain mission, such as the ingress and egress maneuvers. Therefore, in the present study, the design methodology of a BWB UAUV is presented, integrating calculations for the multi-domain needs.

2. Conceptual design methodology

The conceptual design methodology is mainly based on well-established aircraft design textbooks and UAV presizing methods [12, 13], with various considerations stemming from the submarine and UUV design methodologies [14]. An in-house tool was developed, in order to carry out the presizing

calculations for the conceptual layout study. Two different initial concept sketches are displayed in figure 2a while figure 2b presents the roadmap of the in-house tool.

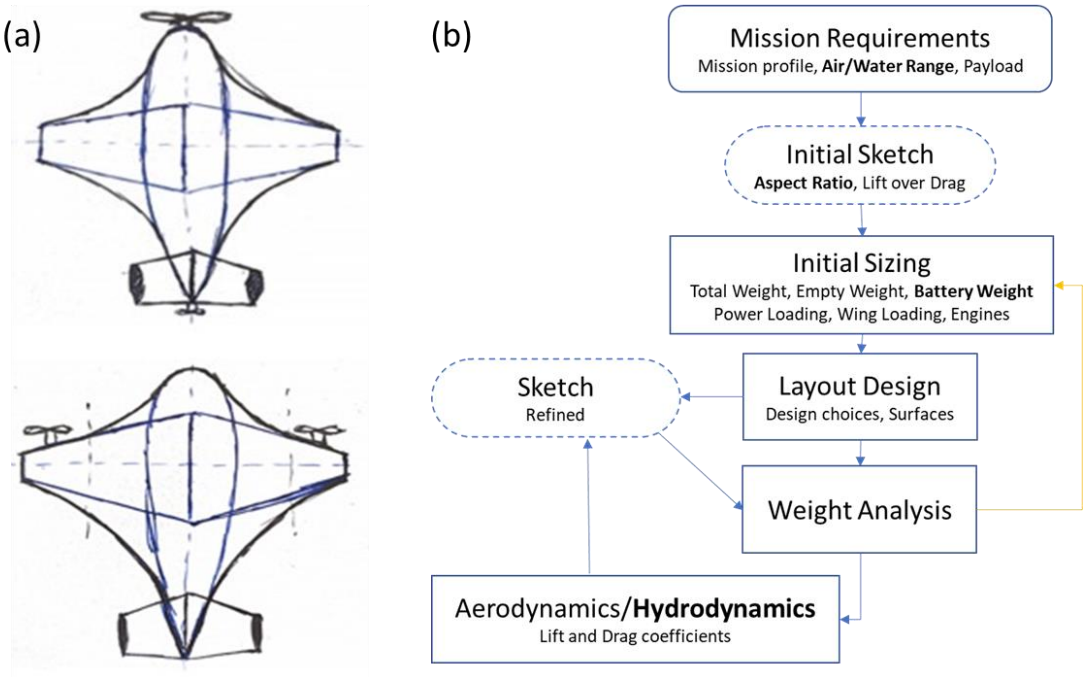

Figure 2. (a) Back of a napkin sketch with different propulsion systems (b) UAUV proposed conceptual design methodology.

2.1. Mission profile and requirements

The first step of the methodology is to specify the platform's mission requirements, for both the aerial and the underwater environment. An extensive investigation of the available literature [3-8] was carried out to set realistic initial requirements for the mission of the UAUV. The top performance characteristics of these prototypes were set as mission requirements for the platform under study (table 1).

Table 1. Mission Requirements for the under-study platform called Flying Manta Ray-1 (FMR-1).

	Air	Water
Range	50 km	25 km
Max Velocity	108 km/h	10,8 km/h
Stall Velocity	43,2 km/h	-
Altitude/Depth	500 m	3 m
Payload	1 kg	
Take Off	Vertical Egress	
Landing	Water surface Landing	

A typical UAUV mission initiates on the water surface near the shore with a vertical takeoff and climb towards the specified flight altitude. Through aerial cruise the vehicle rapidly approaches the desired underwater mission location. At this stage, a loiter may take place in order for the UAUV to accurately initiate the ingress procedure, avoiding unnecessary wave loads. During the underwater cruise and loiter, the main mission takes place (e.g. water sampling, sea mapping, identification of foreign objects) and finally the vehicle takes-off once more to return to base through air cruising.

2.2. *Weight estimation*

The presizing begins with an initial estimation of the aircraft Gross Takeoff Weight (GTOW or W_0), i.e. the aircraft total weight at the start of its mission. For a UAUV it is comprised of the payload weight W_p, the empty weight W_e and, in the case of electric propulsion, the battery weight W_b, so that:

$$W_0 = W_p + W_e + W_b \quad (1)$$

The payload weight refers to the total weight of the on-board electronic and surveillance equipment and is already defined by the mission requirements. The empty weight is estimated from the available historical trends and statistical data [9, 12] of lightweight UAVs. To achieve the desired underwater operating depth, a variable buoyancy method is employed by specifying specific volumes of the platform as ballasts. Regarding the initial estimation of the battery weight and the wing's Aspect Ratio (AR), the available statistical data for UAUVs, presented in figure 3, are used. It can be observed that the AR rarely exceeds the value of 6, and this is attributed mainly to the intense pressure loads from which high AR wings suffer underwater.

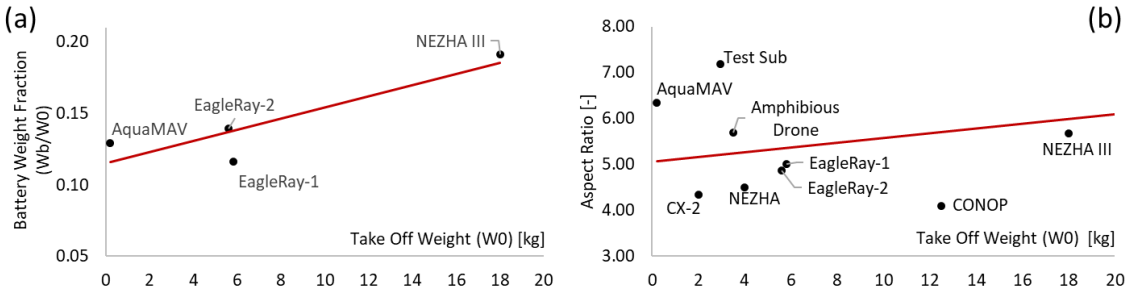

Figure 3. (a) Statistical battery weight fraction estimation (b) Statistical Aspect Ratio estimation.

2.3. *Wing and propulsion system sizing*

After the initial estimation of the takeoff weight, the Thrust-to-Weight ratio (T/W) and wing loading (W/S) have to be calculated. An equivalent term to the thrust-to-weight ratio, that may be used in the case of propeller or buoyancy driven engines, is the power loading, which is the weight of the vehicle divided by the engine horsepower (W/hp). This term is calculated for various mission segments and then the largest value is selected, to ensure that the UAUV has sufficient maximum power. The vertical egress (figure 4) is a highly energy-consuming maneuver and is a crucial part in the mission of UAUVs.

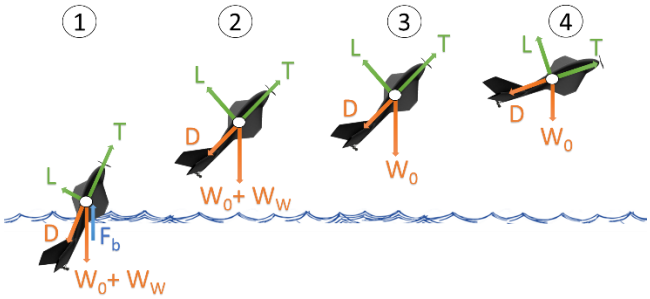

Index	Force
L	Lift
T	Thrust
D	Drag
W_0	Vehicle Weight
W_W	Water Weight
F_b	Buoyancy

Figure 4. Egress stages required for the maximum power calculation.

To the best of the author's knowledge, no presizing expressions concerning the egress power requirements exist in the bibliography. The egress procedure of the under-study platform is selected to be similar to the one demonstrated by Stewart et al. [7] and is divided in 4 stages, as presented in figure 4. At the first stage of the egress, the vehicle is oriented vertically and only the aerial propeller is over the water surface. At the second stage the vehicle is completely out of water, but the wings have not

been drained yet. At the third stage the wings are drained, and the speed is 80% of the stall speed. Finally, at the fourth stage, the vehicle has reached its stall velocity. Further calculations beyond this stage are considered unnecessary, as the UAUV will gradually rotate into horizontal orientation. The physics of vertical egress for a UAUV present some similarity to the hovering and climb of a helicopter. Thus, utilizing the momentum theory that calculates the power required for hover and climb of helicopters [12], and adjusting the variables accordingly for the case of a vertically moving, front mounted propeller vehicle, the authors propose equation (2) to calculate the horsepower required for egress (imperial units required as inputs).

$$P_{hp} = \left(W * \sqrt{\frac{W}{2*\rho*S_{disc}}} + \frac{W*V_{climb}}{2} \right) \frac{1}{550*\eta_{prop}} \quad (2)$$

In table 2, a comparison between the most power demanding mission segments of the UAUV is presented. It can be observed that the required power for vertical egress is slightly more than two times that of a typical rate of climb for a UAV. The maximum power is required during stage 2 of the egress maneuver, when the vehicle is out in the air but with wings still full of water.

Table 2. Power required for various mission segments of the UAUV.

	Maneuver	Max $P_{required}$ [hp]
Air	Vertical Egress	2,55
	Rate of Climb	1,24
	Max velocity	0,35
Water	Max velocity	0,22

2.4. Refined weight estimation

Usually, weight prediction methods for aircrafts and UAVs are based on statistical data and empirical relations derived from conventional configurations [12]. However, the UAUV platform includes many design novelties, such as the BWB layout geometry (figure 5) and the Carbon Fiber Reinforced Polymer (CFRP) manufacturing methods, that have not been integrated in design textbooks yet and may result in a significant weight miscalculation.

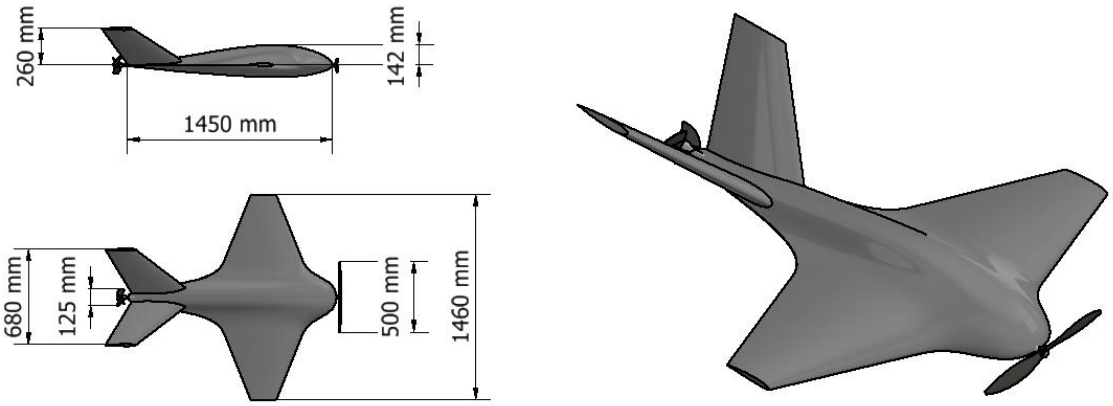

Figure 5. FMR-1 final geometry layout.

Fudge Factors found in related literature [9] are employed to include these novelties in the refined weight estimation. These factors changed the final weight estimation of the vehicle by 15%, a significant deviation that could complicate the preliminary design stage.

3. Aerodynamic and Hydrodynamic Prediction

3.1. Semi-empirical analysis

The calculation of lift and drag coefficients both for the air and for the water are based on Roskam's methodology [15] with the appropriate modifications to account for the BWB unique layout [16]. The external BWB geometry is designed with 3 different airfoil sections. Regarding the lift generation each airfoil has a main area of effect. The Zero-Lift coefficient (C_{L0}) is calculated to include each airfoil's area of effect, while the BWB body is considered as a single trapezoidal wing in this case (equation 3). The BWB layout presents also a reduced interference drag comparing to a conventional tube-and-wing. This is illustrated in the Zero-Lift-Drag coefficient (C_{D0}) calculation (equation 4).

$$C_{L0_{wf}} = C_{L0_{main\ body}} * \frac{S_{mb}}{S_w} + C_{L0_{root}} * \frac{S_{root}}{S_w} + C_{L0_{tip}} * \frac{S_{tip}}{S_w} \quad (3)$$

$$C_{D0_{wf}} = C_{D0_{lofting\ wing}} + C_{D0_{clean\ wing}} \quad (4)$$

3.2. CFD methodology

In order to calibrate and validate the in-house tool for the aerodynamic and hydrodynamic prediction, CFD calculations are performed. The CFD analysis was conducted using the ANSYS Fluent commercial software (ANSYS @ Scientific Research, Release 20.1). An unstructured grid was generated (figure 6), consisting of approximately 10,000,000 computational elements, which is the product of a 5-grid mesh independency study until a 2% difference in the C_D value was reached. In each case, 18 inflation layers were implemented on the walls, the first of which was placed at $1.5x10^{-5}$ m, and resulted in an average y^+ of 1, so that an accurate modeling of the near wall region boundary layer development is achieved, followed by the accurate calculation of the surface shear stresses.

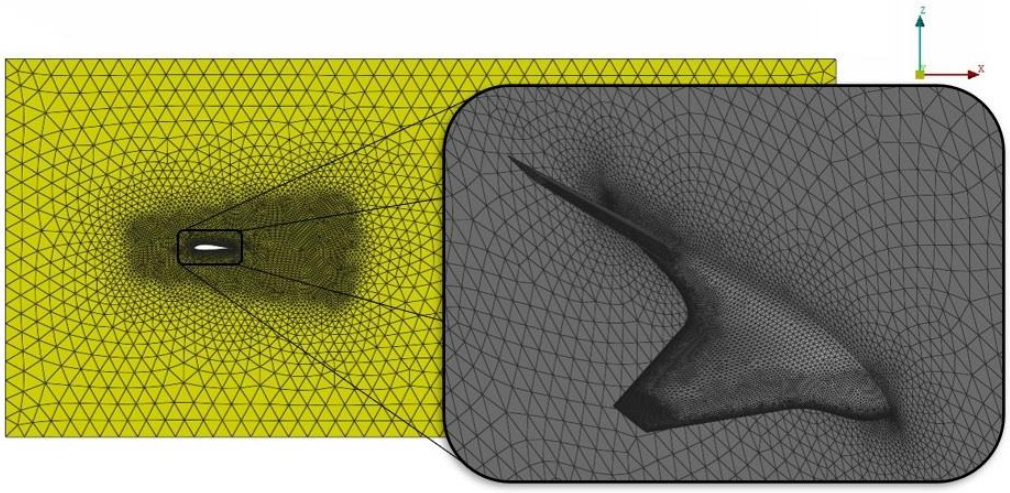

Figure 6. The UAUV computational mesh model.

Regarding the turbulence modelling, a sensitivity analysis was conducted for the two mediums, air and water. The aerial cruise Reynolds is approximately 10^6, a region where Spalart-Allmaras [17] and k-ω SST [18] have both been widely used and validated to be accurate in aircraft applications [9]. The aerial inlet turbulence intensity was set at 1% and the eddy viscosity ratio at 0.2, representing typical flight conditions [9]. The underwater cruise Reynolds number, is approximately $2.5x10^5$, falling in the range of transitional flow. The experimental data for UUVs or submarines is very limited in the available literature, making the validation of turbulence models extremely challenging. This is mostly caused by the difficulty of underwater tunnel experiments, including the direct dependency of the environmental conditions (e.g., wind, waves or water currents' effect). Thus, a comparative study between the

Transitional SST turbulence model [19], which is proposed by the literature as the most accurate in the transitional region [20], Spalart-Allmaras and k-ω SST models is conducted for the water cruise segment. The underwater inlet turbulence intensity was set at 5%, a value derived from experimental data for the cruise depth and average water conditions [21], and the eddy viscosity ratio was set equal to 0.05 [22].

4. Results

The aim of this study was to provide a complete conceptual design methodology, resulting to an accurate low-fidelity aerodynamic and hydrodynamic analysis of the platform. In figure 7, the coefficient of lift shows a good agreement between the semi-empirical tool and the CFD results, both in the air and in the water. The coefficient of drag (figure 8) shows good qualitative agreement in the air, while in the water a deviation appears between the in-house tool and the computational results at negative angles of attack. Quantitatively, the in-house tool seems to have an almost constant offset of about 0.005 from the CFD results in the air and an average of 0.015 in the water. This deviation may occur due to differences in the skin friction calculation of each turbulence model, that leads to an overestimation of the in-house tool's C_D compared to the one from the computational results.

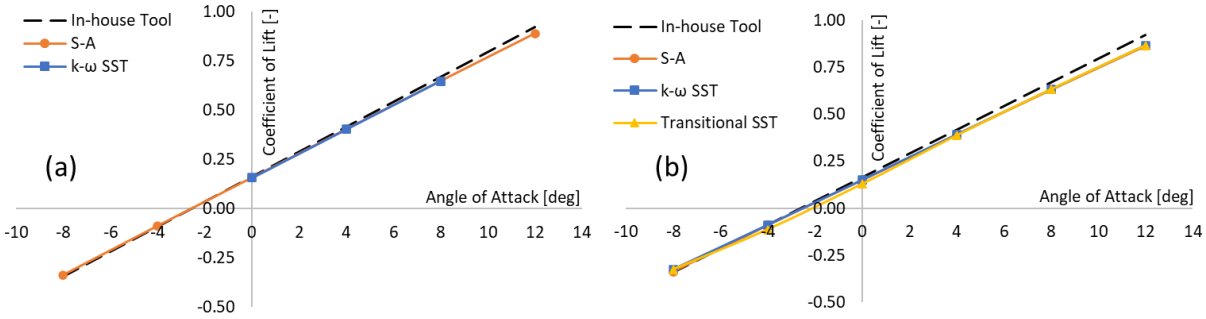

Figure 7. Coefficient of lift for air (a) and for water (b).

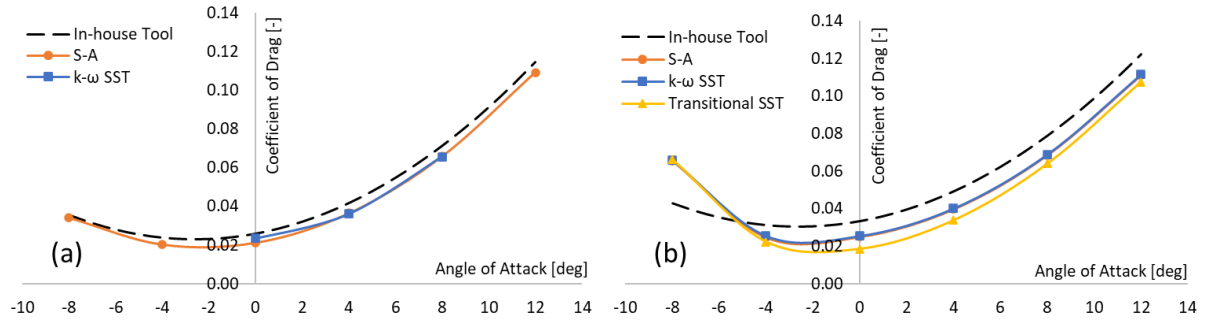

Figure 8. Coefficient of drag for air (a) and for water (b).

The CFD calculations seem to have small differences between the cases with different turbulence models. Thus the 1-equation Spalart-Allmaras model seems to be the most appropriate selection for any further conceptual CFD study in this platform, due to the significantly reduced computational time also, compared to the 2-equation k-ω SST and the 4-equation Transitional SST.

5. Conclusions

In the current study, a complete step-by-step conceptual design methodology for UAUVs is proposed. Aspects of the hybrid mission vehicles, such as the battery sizing or the estimation of the power required for the transition, have also been addressed. The good accordance between the in-house tool and the

high-fidelity CFD calculations, prove the suitability of the proposed methodology as a quick pre-sizing tool. The in-house tool could be further calibrated and constantly updated through the literature's UAUV data. Finally, as a future work, a comparison between a conventional tube-and-wing and a BWB configuration, both sized from the in-house tool, should be conducted to examine more thoroughly the benefits of the BWB platform in the underwater environment.

References

[1] Drews PL, Neto AA and Campos MF (2009) A survey on aerial submersible vehicles. In *Conference: IEEE/OES Oceans* (pp. 4244-2523)
[2] Zimmerman S and Abdelkefi A (2017) Review of marine animals and bioinspired robotic vehicles: classifications and characteristics. *Progress in Aerospace Sciences* **93**
[3] Drews PL, Neto AA and Campos MF (2014) Hybrid unmanned aerial underwater vehicle: modeling and simulation. In *2014 IEEE/RSJ International Conference on Intelligent Robots and Systems* (pp. 4637-4642). IEEE.
[4] Young T Z (2014) Design and testing of an unmanned aerial to underwater vehicle. In *Proc. 14th AIAA Aviation Technol., Integr., Oper. Conf.*
[5] Siddall R and Kovac M (2016) Fast aquatic escape with a jet thruster. *IEEE/ASME Transactions on Mechatronics*, **22(1)**, (pp. 217-226).
[6] Siddall R, Ortega Ancel A and Kovač M (2017) Wind and water tunnel testing of a morphing aquatic micro air vehicle. *Interface focus*, **7(1)**, 20160085.
[7] Stewart W et al (2018) Design and demonstration of a seabird-inspired fixed-wing hybrid UAV-UUV system. *Bioinspiration & biomimetics*, **13(5)**, 056013.
[8] Lu D et al. (2021) Design, fabrication, and characterization of a multimodal hybrid aerial underwater vehicle. *Ocean Engineering*, *219*, 108324.
[9] Panagiotou P, Fotiadis-Karras S and Yakinthos K (2018) Conceptual design of a blended wing body MALE UAV. *Aerospace Science and Technology*, **73**, (pp. 32-47).
[10] Crouse G (2010) Conceptual design of a submersible airplane. In *48th AIAA Aerospace Science Meeting Including the New Horizons Forum and Aerospace Exposition* (pp. 1012).
[11] Dinelli C, Fisher J, Herkenhoff B and Hassanalian M (2020) Design of a Hybrid Detachable Amphibious Drone for Monitoring Marine Environment. In *AIAA Prop. and En. Forum*
[12] Raymer D P (2018) Aircraft design: a conceptual approach (AIAA Education Series).
[13] Anderson J D (1999) Aircraft performance & design. McGraw-Hill Science Engineering.
[14] Dhanak M R and Xiros N I (2016) *Springer handbook of ocean engineering*. Springer.
[15] Roskam J (1987) Preliminary calculation of aerodynamic, thrust and power characteristics. *Airplane design*, **21**, (pp. 213-354).
[16] Papadopoulos C, Mitridis D and Yakinthos K. (2021) Conceptual design of a novel Unmanned Ground Effect Vehicle. In *IOP Conf. Series: Mat. Sci. and Eng.* 1024 (pp. 012058)
[17] Spalart P and Allmaras S (1992) A one-equation turbulence model for aerodynamic flows. In *30th Aerospace sciences meeting and exhibit* (pp. 439).
[18] Menter F R (1994). Two-equation eddy-viscosity turbulence models for engineering applications. *AIAA journal*, **32(8)**, 1598-1605.
[19] Menter F R, Langtry R B, Likki S R, Suzen Y B, Huang P G and Völker, S. (2006). A correlation-based transition model using local variables—part I: model formulation.
[20] Papadopoulos C, Katsiadramis V and Yakinthos K (2019) Numerical 3D study on the influence of spanwise distribution of tubercles on wings for UAV applications. In *MATEC Web of Conferences* **304** (pp. 02014). EDP Sciences.
[21] Mycek P, Gaurier B, Germain G, Pinon G and Rivoalen E (2014) Experimental study of the turbulence intensity effects on marine current turbines behaviour. Part I: One single turbine. *Renewable Energy*, **66**, (pp. 729-746).
[22] Rumsey C L and Spalart P R (2009) Turbulence model behavior in low Reynolds number regions of aerodynamic flowfields. *AIAA journal*, **47(4)**, (pp. 982-993).